



P. Decuzzi, Ph.D.

PATIENT-SPECIFIC COMPUTATIONAL MODELING AND MAGNETIC NANOCONSTRUCTS: TOOLS FOR MAXIMIZING THE EFFICACY OF STEM CELL-BASED THERAPIES

Paolo Decuzzi, Ph.D.

Houston Methodist Hospital Research Institute, Houston Methodist Hospital, Houston, Texas

Abstract

Stem cell transplantation has the potential to restore heart function following myocardial infarction. However, the success of any stem cell-based therapy is critically linked to the effective homing and early engraftment of the injected cells at the infarcted site. Here, a hierarchical multiscale computational model is proposed for predicting the patient-specific vascular transport and intratissue homing and migration of stem cells injected either systemically or locally. Starting with patient-specific data, such as the vascular geometry, blood flow, and location of the infarcted area, the computational model can be used to perform parametric analysis to identify optimal injection conditions in terms of administration route, injection site, catheter type, and infusion velocity. In addition to this, a new generation of magnetic nanoconstructs is introduced for labeling stem cells and monitoring their behavior in vivo via magnetic resonance imaging. These nanoconstructs also can be used for multimodal imaging, merging MRI and nuclear imaging, and the intracellular delivery of active agents to support stem cell differentiation. The convergence of computational modeling and novel nanoconstructs for stem cell labeling could improve our understanding in cell homing and early engraftment at the infarcted site and thus pave the way to more effective stem cell-based therapies.

Introduction

Although the number of deaths from cardiovascular diseases (CVD) has steadily decreased over the last 40 years, the morbidity associated with nonfatal CVD, consequent disability, and decreased quality of life is still a huge burden on society and the leading cause of medical expenses in most developed countries.¹ Hypertension and coronary artery disease, the two major types of CVD, can both lead to myocardial infarction (MI), inducing interruption of blood supply and, consequently, local tissue damage, death of cardiomyocytes, and eventually heart failure. Since the heart has limited regenerative capacity, the damaged tissues tend to become a collagen scar exhibiting biophysical properties that are significantly different from the original tissue.^{2,3} Depending on the extension of the damaged area, the presence of scar tissue may alter the function of the heart and potentially induce life-threatening arrhythmias and aneurysms. There is clearly a need for improvement in the current methods for preventing and limiting the recurrence of CVD and for regenerating the tissue that has been irreversibly damaged.

Undifferentiated or partially differentiated cells, the so-called stem cells, are distributed throughout our body in different organs and are involved in tissue repair at the damaged site.^{4,7} In the infarcted zone, these cells are believed to induce and support regeneration by differentiating into new cardiomyocytes,^{8,9} stimulating the formation of new blood vessels to increase the local intake of nutrients and oxygen,⁵ and secreting specific factors to facilitate cell growth and the recruitment of other stem cells.⁹ However, the amount of resident stem cells is limited, and their recruitment at the site of damage is generally insufficient for effective restoration of the tissue. Therefore, stem

cell transplantation in patients following myocardial infarction has been proposed as a possible effective therapy.^{7,10-12} This transplantation can be done by injecting stem cells, or mixtures of stem cells and polymeric matrices, either locally or systemically via intravascular administration.

Different approaches have been proposed for stem cell transplantation, and different types of stem cells have been used in preclinical and clinical models. At least three major routes of administration have been tested: direct intramyocardial injection upon thoracotomy;¹³⁻¹⁵ catheter-based coronary arteries and venous administration;¹⁶⁻¹⁹ and systemic intravenous injection.^{20,21} Each of these delivery approaches has advantages and disadvantages, and the most effective choice depends on the location and extension of the infarcted area; it is indeed patient specific. A multitude of cell types have been proposed for repairing the infarcted tissue, including pluripotent stem cells such as embryonic stem cells and induced pluripotent stem cells,^{5,22,23} and adult stem cells such as skeletal myoblasts, bone marrow stem cells, mesenchymal stem cells, and in situ fibroblast reprogramming.^{24,25}

The success of any stem cell-based therapy is critically linked to the effective homing at the infarcted site and integration with the surrounding microenvironment of the injected cells. In order to replicate and transform into cardiomyocytes, the transplanted stem cells need to reach the diseased tissue in a sufficiently high dose, reside within the infarcted area for a sufficiently long time, and be vital and sufficiently nourished by oxygen and other nutrients. The route of administration and the complexity of the vascular structure in the vicinity of the damaged area, as well as the type of stem cell, are all critical factors in defining the transplant success. This manuscript presents a computational modeling tool

and imaging nanoconstructs that can be synergistically used to personalize and optimize the transplantation of stem cells on a patient-specific basis.

Computational Modeling in Stem Cell Transplantation

The vascular transport and tissue accumulation of injected stem cells is a complex multiscale and multiphysics problem that subsumes molecular, subcellular, cellular, and supracellular events developing over time scales ranging from milliseconds to hours and days. In the case of systemic administration, which is by far the less invasive route of transplantation, a solution containing the stem cells or stem cells mixed with an injectable polymeric paste is released into the lumen, where it interacts with the fast-moving red blood cells (RBCs), molecules dispersed in the plasma, and endothelial cells lining the vessel walls. As the injected solution is carried downstream by blood flow, some of the stem cells are pushed laterally towards the vessel wall, can recognize and adhere to the damaged endothelium near the infarcted area—aided by their membrane receptor molecules—and, eventually, can migrate into and colonize the damaged tissue. This complex process, schematically depicted in Figure 1, can be broken down in three major events: (1) vascular transport of stem cells; (2) near-wall dynamics and vascular adhesion of stem cells; and (3) intratissue migration of stem cells.

Over the years, the author and his collaborators have developed a hierarchical computational model to predict the wall and tissue accumulation of injectable agents, such as circulating cells, nanoparticles, and small and macromolecules.²⁶⁻³⁶ This hierarchical computational model comprises three modules, each focusing on different scales and biological compartments. The first module deals with the macroscopic transport of the stem cell solution in patient-specific vascular networks (Figure 1A); the second module analyzes the near-wall dynamics and blood vessel wall adhesion of the injected solution of stem cells (Figure 1B); and the third module focuses on the transport in the extravascular space and migration within the damaged tissue of the injected stem cells (Figure 1C). The modules are all connected together so that information can be transferred efficiently and accurately over multiple temporal and spatial scales but can also be used separately depending on the aim of the study.

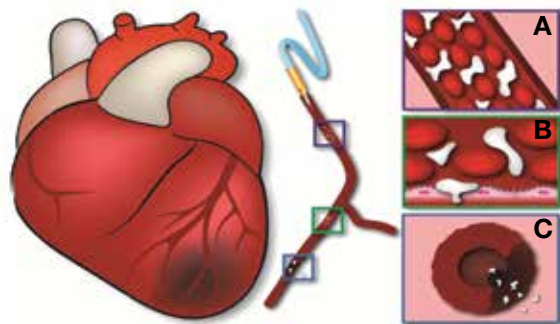


Figure 1. The vascular transport of stem cells, from the site of injection to the damaged area, can be broken down in three major steps: (1) vascular transport of stem cells; (2) near-wall dynamics and vascular adhesion of stem cells; and (3) intratissue migration of stem cells. Computational modules have been developed for each of these steps and integrated in a single hierarchical multiscale computational tool.

Module 1: Vascular Transport of Stem Cells

Blood flow and vascular transport are influenced by authentic, patient-specific vascular geometry and endothelial wall properties. A critical step in developing accurate predictive tools is the precise reconstruction of the vascular geometry, from the site of injection to the infarcted area, using magnetic resonance imaging (MRI) or computed tomography.³⁶ This requires preprocessing for improving the quality of the clinical images, geometrical segmentation, and solid and mesh constructions for the computational analysis. The resulting three-dimensional (3D) vascular geometry is then used for solving the transport problem by coupling a Navier-Stokes solver for the blood flow with a linear scalar advection-diffusion equation for studying the time-dependent evolution of the system.³⁴ Following this approach, the temporal and spatial distribution of several biophysical parameters—such as the wall shear rate (WSR), wall shear stress (WSS), oscillatory index (OSI), velocity profile, pressure field, and volumetric concentration of any injected agents—can be predicted within the authentic, patient-specific vascular network.³⁴ Figure 2A shows the sequential steps required for predicting the local flow dynamics and vascular deposition of injected agents in patients affected by peripheral arterial disease, for example. First, the MR image of the individual's superficial femoral artery (SFA) is acquired over the vessel length; then the images are segmented; finally, the SFA is reconstructed in 3D and, eventually, imported in a finite element solver where the actual simulations for blood flow and injected agent transport are performed. Indeed, this approach is general and can be applied to any vascular district. For instance, Figure 2B shows the vascular deposition (surface concentration) upon specific wall adhesion of agents injected via a catheter in a coronary artery. In all simulations, the inlet blood velocity profiles are quantified via time of flight (TOF) magnetic resonance angiography (MRA). The distinctive advantage of computational analysis is that the simulations can be run for different initial conditions for the same patient data. In other words, the location, orientation, infusion velocity, and geometry of the catheter as well as the properties of the injected stem cell solution can be virtually changed to identify the optimal interventional strategy for the specific individual.

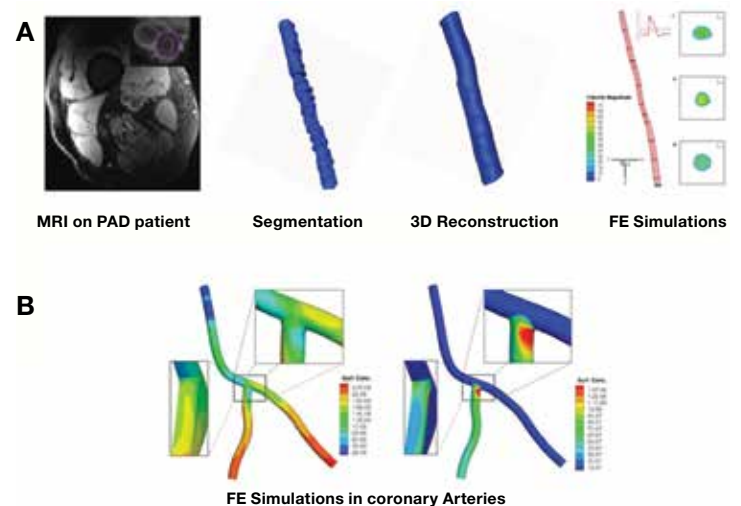


Figure 2. (A) MR image of the superficial femoral artery (SFA) of a patient affected by peripheral; segmentation of the MR images; 3D reconstruction of the SFA; finite element simulation on the patient-specific SFA. (B) Wall surface concentration of intra-arterially injected agents using a catheter placed in a patient-specific coronary artery.

Module 2: Near-Wall Dynamics and Vascular Adhesion of Stem Cells

Blood is a complex fluid composed of an aqueous solution, rich in proteins and molecules (plasma), in which different types of cells are suspended (leukocytes, erythrocytes and platelets). Erythrocytes, or RBCs, are by far the most abundant, with 4- to 6-million cells per microliter of human blood, and constitute 35% to 45% of the total blood volume. The vascular transport of molecules and small nanoparticles (≤ 100 nm) is not affected by the presence of RBCs.²⁹ Conversely, cells and submicron-sized particles do interfere with the circulating RBCs, and their near-wall dynamics is significantly influenced by the presence of other blood cells.^{31,32} Therefore, in modeling the near-wall dynamics and vascular adhesion of stem cells, the presence of RBCs cannot be neglected. The computational Module 2 allows us to predict the near-wall behavior of the injected stem cells while they are repeatedly interacting with the fast moving and abundant RBCs. Figure 3A shows a typical simulation set-up where a cylindrical vessel is filled with plasma and RBCs up to about 40% of the lumen volume. Here, RBCs are modeled as biconcave vesicles with a hyperelastic membrane containing an aqueous solution.³⁷ In the same image, a stem cell (white globe) is also depicted surrounded by the RBCs. Representative snapshots for the fluid dynamic simulation (Figure 3B) show how the stem cell, while it is transported downstream by the flow, is pushed laterally by the RBCs and squeezed against the vessel walls, where it eventually firmly adheres. Figure 3C depicts the trajectory of the cell as it moves closer to the wall, reducing the separation distance δ . Figure 3D shows the complexity of the blood flow and stream lines in the presence of RBCs and stem

cells. Indeed, the lateral motion and pushing against the wall is mostly induced by the presence of the RBCs. The adhesion of the stem cells to the endothelium is modeled using a multiscale approach, where the hydrodynamic forces exerted over the cell are balanced by adhesive forces originating at the interface. The adhesive forces include both nonspecific colloidal interactions (van der Waals, electrostatic, and steric) and specific ligand (L)-receptor (R) molecular interactions regulated by the forward k_f and reverse k_r reaction rates ($L + R \rightleftharpoons LR$).^{28,38} This module allows us to predict the probability of adhesion of a stem cell to the vessel wall that can then be integrated in the previous computational module to quantify the overall vessel wall distribution of the injected stem cells in the patient-specific vascular geometry. This information can be used to predict the percentage of stem cells that would home within the infarcted area as a function of the initial injection conditions.

Module 3: Intra-Tissue Migration of Stem Cells

The extravascular dynamics of the stem cells is rooted in the way these cells interact with the surrounding microenvironment and integrate on the multiple biophysical stimuli (chemotaxis, haptotaxis, and durotaxis). We have successfully used a cellular Potts model to study the migration and spatiotemporal organization of cell clusters within 3D tissue matrices (Figure 4).³³ This approach combines a discrete stochastic model for the motion of individual cells with a deterministic model based on a set of differential equations for predicting the spatiotemporal distribution of biophysical stimuli within the tissue matrix. The computational module uses the principle of energy minimization to compute the equilibrium configuration

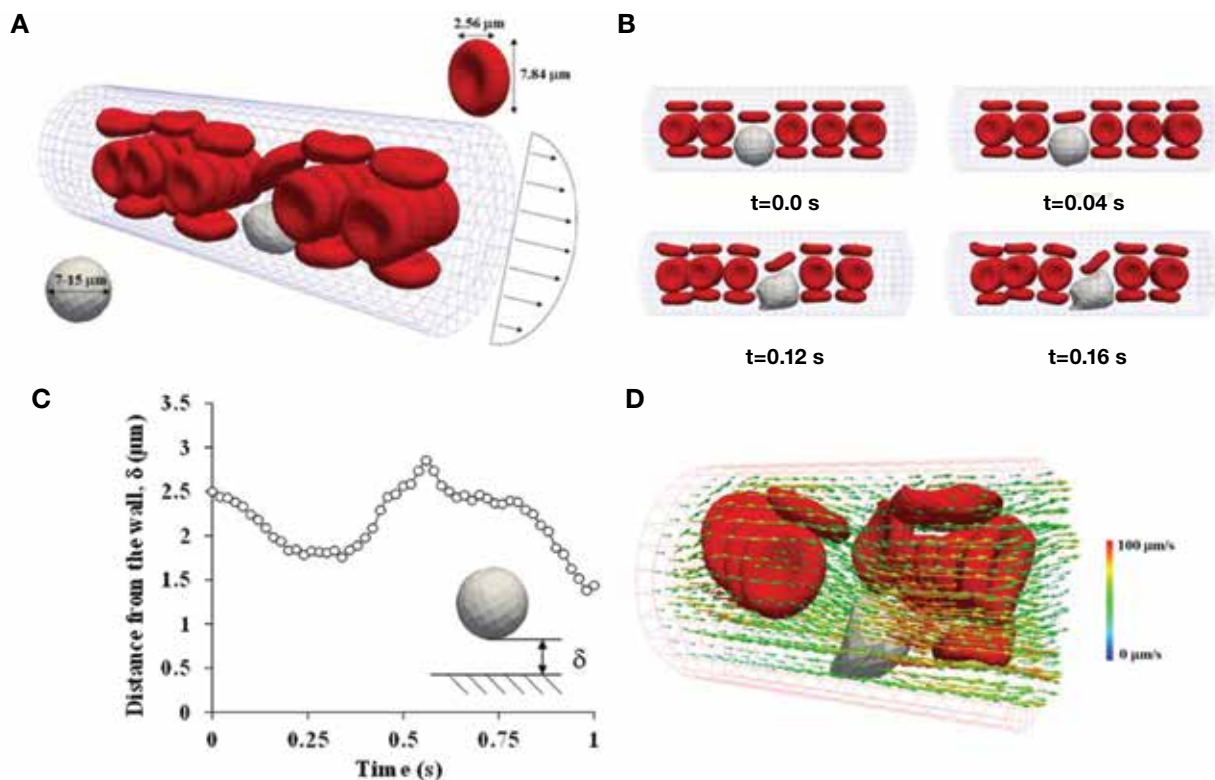


Figure 3. (A) The typical computational set-up for the analysis of the near wall dynamics of stem cells (white globe) interacting with red blood cells (RBCs). (B) Representative snapshots derived from the fluid dynamic simulation showing the stem cell deformation and interaction with the vessel wall. (C) The trajectory of a stem cell presented as the variation of its separation distance δ from the wall. (D) The complexity of the blood flow and stream lines around RBCs and stem cells.

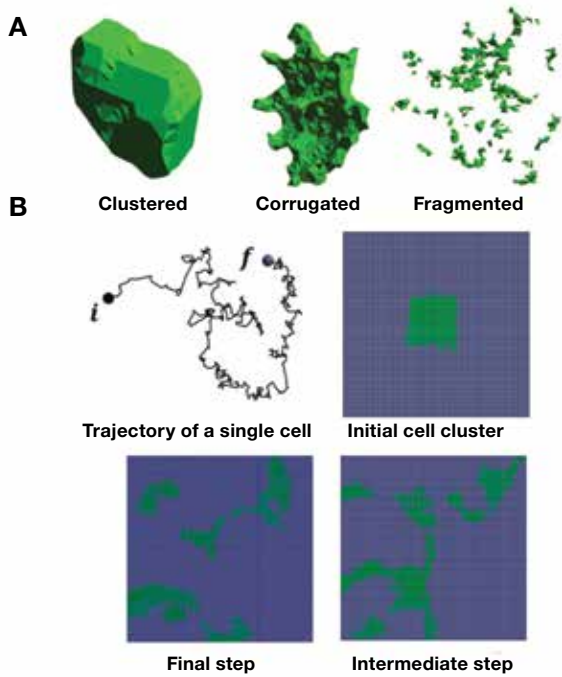


Figure 4. (A) The morphological configuration of a cluster of stem cells injected directly into the damaged area depends on local microenvironmental cues. (B) A representative trajectory of an individual cell and 2D representation of the spatiotemporal evolution of a cell cluster.

of a cluster of cells. It includes information on cell adhesion, cell deformation, cell chemotaxis, haptotaxis, durotaxis, and cell growth as well as the cell response to external biophysical stimuli, such as the spatiotemporal concentrations of nutrients and soluble factors. Therefore, the actual location and migration of the stem cells is predicted as a function of multiple biophysical cues, as driven by the surrounding microenvironment and external stimuli. The model can account for the co-presence of multiple cell types. With this computational tool, parametric analysis can be performed to elucidate the relative importance of cell population density (i.e., local concentration of stem cells); chemotaxis, haptotaxis, durotaxis; cell motility; and adhesion in affecting the migratory properties of the cells. Figure 4A exemplifies the temporal evolution of a cluster of cells as they reorganize themselves to attain different morphologies (clustered, corrugated, and fragmented) as a function of the actual microenvironmental cues. Note that an originally compact cluster of stem cells can, over time, assume a fragmented morphology with cells migrating away from the site of injection depending on the integration of the stem cells with the surrounding tissue. This is even more clearly depicted in Figure 4B, which provides a 2D representation of the cell cluster at three different time points. Also, a representative trajectory of a cell within the cluster is shown. This computational module can also be used independently from the other two for estimating the organization and growth of stem cells that have been directly injected within the damaged site upon thoracotomy.

Magnetic Nanoconstructs in Stem Cell Transplantation

In preclinical and clinical practice, superparamagnetic iron oxide nanoparticles (SPIOs) have been proposed for cell labeling and noninvasive tracking in vivo using MRI.³⁹⁻⁴³ SPIOs are made out of iron oxide crystals and exhibit high T_2 contrast enhancement,

generally increasing with their aggregation and internalization into cells. Stem cells can be labeled with SPIOs ex vivo, before injection, either via magnetofection or magnetoelectroporation.^{44, 45} SPIO-labeled stem cells can provide a means of determining whether the stem cells have reached the infarcted area, how long they remain in the area, and insights into the preferred sites of engraftment. Indeed, SPIO-labeling of stem cells can be used to optimize the injection conditions and the accuracy of the computational tools in preclinical models.

We have developed three different SPIOs-based nanoconstructs that could be used for in vivo stem cell labeling. They are different in size, shape, surface, and material properties, as presented in Figure 5. The hybrid nanoparticles (HNP) present a spherical shape with a diameter of 150 nm and are made out of a poly(L-lactide-co-glycolide) (PLGA) core, incorporating the SPIOs, and a lipid/polymer coating. The mesoporous silicon particles exhibit a discoidal shape and a characteristic size of 1,000 x 400 nm, and the SPIOs are loaded into the mesopores.⁴⁶ Finally, the discoidal polymeric nanoconstructs (DPN) also have a characteristic size of 1,000 x 400 nm but are composed of a mixture of PLGA and PEG that makes them deformable.⁴⁷ The SPIOs are confined within the polymeric matrix and have shown a huge enhancement in transversal relaxivity r_2 ($\sim 800 \text{ mM}^{-1}\text{s}^{-1}$) as compared with commercially available SPIOs. Figure 5c depicts phantom images obtained for the DPNs using a 3T MRI clinical scanner. All three nanoconstructs incorporate ultrasmall SPIOs with a 5 nm metallic core that is, eventually, degraded and metabolized by the cells without any significant toxicity.

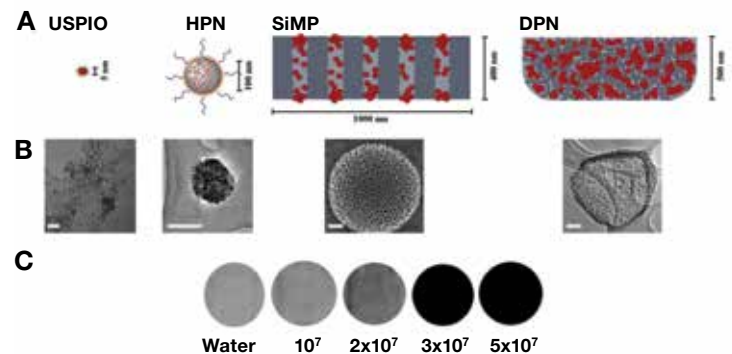


Figure 5. (A) Graphical representation of a 5-nm superparamagnetic iron oxide nanoparticle (SPIO); a 150-nm hybrid nanoparticle (HNP); discoidal 1,000 x 400 nm mesoporous silicon particle (SiMP); and a discoidal 1,000 x 400 nm polymeric nanoconstructs (DPN). (B) Electron microscopy images for the particles listed above. (C) Phantom images for the DPN obtained in a 3T MRI clinical scanner.

Note that in stem cell labeling, it is very important to have access to different nanotechnological platforms in that the nanoconstructs per se can affect the cell behavior.⁴⁸ Importantly, these nanoconstructs can be remotely manipulated via static magnetic fields because of their huge content in magnetic material (about 100 fg of iron per DPN) and can release directly inside the stem cell molecular agents for stimulating and controlling cell differentiation. Moreover, these nanoconstructs can be labeled with

radionucleotides, thus merging together MRI and nuclear imaging, which could help in assessing cell functionality and viability in addition to cell tracking.⁴⁹

Conclusions

The efficiency of stem cell homing within the infarcted tissue can be predicted using patient-specific computational modeling as a function of the vascular geometry, blood flow conditions, and location of the infarcted area. Multifunctional magnetic nanoconstructs can serve to spatially and temporally track the injected stem cells and test for their viability. The combination of computational modeling and sophisticated nanoconstructs for cell labeling should pave the way to new clinical trials for cell-based therapies in cardiovascular disease.

Acknowledgements

The author would like to thank Dr. T.R. Lee, Dr. J. Singh, Dr. S. Hossain, and Mr. M. Landry at Houston Methodist Hospital Research Institute for helping with the figures and data generation. The author acknowledges the collaboration with Dr. T.J.R. Hughes at The University of Texas, Austin, and with Dr. W.K. Liu at Northwestern University for the development of the computational module 1 and 2, respectively. The patient-specific data on PAD were kindly provided by Dr. D. Shah at the Houston Methodist DeBakey Heart & Vascular Center and Dr. G. Bruner at Baylor College of Medicine.

Conflict of Interest Disclosure: The author has completed and submitted the *Methodist DeBakey Cardiovascular Journal* Conflict of Interest Statement and none were reported.

Funding/Support: The author has no funding disclosures.

Keywords: computational modeling, magnetic nanoconstructs, cardiomyocytes, stem cell transplantation

References

1. Roger VL, Go AS, Lloyd-Jones DM, Benjamin EJ, Berry JD, Borden WB, et al. Heart disease and stroke statistics—2012 update: a report from the American Heart Association. *Circulation*. 2012 Jan 3;125(1):e2-e220.
2. Pfeffer JM, Pfeffer MA, Fletcher PJ, Braunwald E. Progressive ventricular remodeling in rat with myocardial infarction. *Am J Physiol*. 1991 May;260(5 Pt 2):H1406-14.
3. Colucci WS. Molecular and cellular mechanisms of myocardial failure. *Am J Cardiol*. 1997 Dec 4;80(11A):15L-25L.
4. Deb A, Wang S, Skelding KA, Miller D, Simper D, Caplice NM. Bone marrow-derived cardiomyocytes are present in adult human heart: A study of gender-mismatched bone marrow transplantation patients. *Circulation*. 2003 Mar 11;107(9):1247-9.
5. Leeper NJ, Hunter AL, Cooke JP. Stem cell therapy for vascular regeneration: adult, embryonic, and induced pluripotent stem cells. *Circulation*. 2010 Aug 3;122(5):517-26.
6. Collins SD, Baffour R, Waksman R. Cell therapy in myocardial infarction. *Cardiovasc Revasc Med*. 2007 Jan-Mar;8(1):43-51.
7. Dimmeler S, Burchfield J, Zeiher AM. Cell-based therapy of myocardial infarction. *Arterioscler Thromb Vasc Biol*. 2008 Feb;28(2):208-16.
8. Caspi O, Huber I, Kehat I, Habib M, Arbel G, Gepstein A, et al. Transplantation of human embryonic stem cell-derived cardiomyocytes improves myocardial performance in infarcted rat hearts. *J Am Coll Cardiol*. 2007 Nov 6;50(19):1884-93.
9. Tateishi K, Takehara N, Matsubara H, Oh H. Stemming heart failure with cardiac- or reprogrammed-stem cells. *J Cell Mol Med*. 2008 Dec;12(6A):2217-32.
10. Erbs S, Linke A, Schächinger V, Assmus B, Thiele H, Diederich KW, et al. Restoration of microvascular function in the infarct-related artery by intracoronary transplantation of bone marrow progenitor cells in patients with acute myocardial infarction: the Doppler Substudy of the Reinfusion of Enriched Progenitor Cells and Infarct Remodeling in Acute Myocardial Infarction (REPAIR-AMI) trial. *Circulation*. 2007 Jul 24;116(4):366-74.
11. Schächinger V, Erbs S, Elsässer A, Haberbosch W, Hambrecht R, Hölschermann H, et al. Intracoronary bone marrow-derived progenitor cells in acute myocardial infarction. *N Engl J Med*. 2006 Sep 21;355(12):1210-21.
12. Psaltis PJ, Zannettino AC, Worthley SG, Gronthos S. Concise review: mesenchymal stromal cells: potential for cardiovascular repair. *Stem Cells*. 2008 Sep;26(9):2201-10.
13. Patel AN, Geffner L, Vina RF, Saslavsky J, Urschel HC Jr, Kormos R, et al. Surgical treatment for congestive heart failure with autologous adult stem cell transplantation: a prospective randomized study. *J Thorac Cardiovasc Surg*. 2005 Dec;130(6):1631-8.
14. Pompilio G, Steinhoff G, Liebold A, Pesce M, Alamanni F, Capogrossi MC, et al. Direct minimally invasive intramyocardial injection of bone marrow-derived AC133+ stem cells in patients with refractory ischemia: preliminary results. *Thorac Cardiovasc Surg*. 2008 Mar;56(2):71-6.
15. Wu KH, Han ZC, Mo XM, Zhou B. Cell delivery in cardiac regenerative therapy. *Ageing Res Rev*. 2012 Jan;11(1):32-40.
16. Sherman W, Martens TP, Viles-Gonzalez JF, Siminiak T. Catheter-based delivery of cells to the heart. *Nat Clin Pract Cardiovasc Med*. 2006 Mar;3 Suppl 1:S57-64.
17. Silva GV, Perin EC, Dohmann HF, Borojevic R, Silva SA, Sousa AL, et al. Catheter-based transendocardial delivery of autologous bone-marrow-derived mononuclear cells in patients listed for heart transplantation. *Tex Heart Inst J*. 2004;31(3):214-9.
18. Lederman RJ, Guttman MA, Peters DC, Thompson RB, Sorger JM, Dick AJ, et al. Catheter-based endomyocardial injection with real-time magnetic resonance imaging. *Circulation*. 2002 Mar 19;105(11):1282-4.
19. Fuchs S, Baffour R, Zhou YF, Shou M, Pierre A, Tio FO, et al. Transendocardial delivery of autologous bone marrow enhances collateral perfusion and regional function in pigs with chronic experimental myocardial ischemia. *J Am Coll Cardiol*. 2001 May;37(6):1726-32.
20. Thompson CA, Nasser BA, Makower J, Houser S, McGarry M, Lamson T, et al. Percutaneous transvenous cellular cardiomyoplasty. A novel nonsurgical approach for myocardial cell transplantation. *J Am Coll Cardiol*. 2003 Jun 4;41(11):1964-71.
21. Halkos ME, Zhao ZQ, Kerendi F, Wang NP, Jiang R, Schmarkey LS, et al. Intravenous infusion of mesenchymal stem cells enhances regional perfusion and improves ventricular function in a porcine model of myocardial infarction. *Basic Res Cardiol*. 2008 Nov;103(6):525-36.

22. Okita K, Ichisaka T, Yamanaka S. Generation of germline-competent induced pluripotent stem cells. *Nature*. 2007 Jul 19;448(7151):313-7.
23. Wernig M, Meissner A, Foreman R, Brambrink T, Ku M, Hochedlinger K, et al. In vitro reprogramming of fibroblasts into a pluripotent ES-cell-like state. *Nature*. 2007 Jul 19; 448(7151):318-24.
24. Silva GV, Litovsky S, Assad JA, Sousa AL, Martin BJ, Vela D, et al. Mesenchymal stem cells differentiate into an endothelial phenotype, enhance vascular density, and improve heart function in a canine chronic ischemia model. *Circulation*. 2005 Jan 18;111(2):150-6.
25. Kinnaird T, Stabile E, Burnett MS, Shou M, Lee CW, Barr S, et al. Local delivery of marrow-derived stromal cells augments collateral perfusion through paracrine mechanisms. *Circulation*. 2004 Mar 30;109(12):1543-9.
26. Decuzzi P, Lee S, Decuzzi M, Ferrari M. Adhesion of microfabricated particles on vascular endothelium: a parametric analysis. *Ann Biomed Eng*. 2004 Jun;32(6): 793-802.
27. Decuzzi P, Lee S, Bhushan B, Ferrari M. A theoretical model for the margination of particles within blood vessels. *Ann Biomed Eng*. 2005 Feb;33(2):179-90.
28. Decuzzi P, Ferrari M. The adhesive strength of non-spherical particles mediated by specific interactions. *Biomaterials*. 2006 Oct;27(30):5307-14.
29. Decuzzi P, Causa F, Ferrari M, Netti PA. The effective dispersion of nanovectors within the tumor microvasculature. *Ann Biomed Eng*. 2006 Apr;34(4):633-41.
30. Decuzzi P, Ferrari M. The receptor-mediated endocytosis of nonspherical particles. *Biophys J*. 2008 May 15;94(10): 3790-7.
31. Lee SY, Ferrari M, Decuzzi P. Shaping nano-/micro-particles for enhanced vascular interaction in laminar flows. *Nanotechnology*. 2009 Dec 9;20(49):495101.
32. Lee SY, Ferrari M, Decuzzi P. Design of bio-mimetic particles with enhanced vascular interaction. *J Biomech*. 2009 Aug 25;42(12):1885-90.
33. Singh J, Hussain F, Decuzzi P. Role of differential adhesion in cell cluster evolution: from vasculogenesis to cancer metastasis. *Comput Methods Biomech Biomed Engin*. 2013 May 8.
34. Hossain SS, Zhang Y, Liang X, Hussain F, Ferrari M, Hughes TJ, et al. In silico vascular modeling for personalized nanoparticle delivery. *Nanomedicine (Lond)*. 2013 Mar;8(3): 343-57.
35. Zhang L, Gerstenberger A, Wang X, Liu WK. Immersed finite element method. *Comput Method Appl Mech Eng*. 2004 May 28;193(21-22):2051-67.
36. Hughes TJR, Cottrell JA, Bazilevs Y. Isogeometric analysis: CAD, finite elements, NURBS, exact geometry and mesh refinement. *Comput Method Appl Mech Eng*. 2005 Oct 1; 194(39-41):4135-95.
37. Liu WK, Liu Y, Farrell D, Zhang L, Wang XS, Fukui Y, et al. Immersed finite element method and its applications to biological systems. *Comput Method Appl Mech Eng*. 2006 Feb 15;195(13-16):1722-49.
38. Decuzzi P, Ferrari M. Design maps for nanoparticles targeting the diseased microvasculature. *Biomaterials*. 2008 Jan;29(3):377-84.
39. Bulte JW, Arbab AS, Douglas T, Frank JA. Preparation of magnetically labeled cells for cell tracking by magnetic resonance imaging. *Methods Enzymol*. 2004;386:275-99.
40. Cao F, Lin S, Xie X, Ray P, Patel M, Zhang X, et al. In vivo visualization of embryonic stem cell survival, proliferation, and migration after cardiac delivery. *Circulation*. 2006 Feb 21;113(7):1005-14.
41. Bulte JW, Kraitchman DL. Iron oxide MR contrast agents for molecular and cellular imaging. *NMR Biomed*. 2004 Nov;17(7):484-99.
42. Caruthers SD, Neubauer AM, Hockett FD, Lamerichs R, Winter PM, Scott MJ, et al. In vitro demonstration using 19F magnetic resonance to augment molecular imaging with paramagnetic perfluorocarbon nanoparticles at 1.5 Tesla. *Invest Radiol*. 2006 Mar;41(3):305-12.
43. Foster-Gareau P, Heyn C, Alejski A, Rutt BK. Imaging single mammalian cells with a 1.5 T clinical MRI scanner. *Magn Reson Med*. 2003 May;49(5):968-71.
44. Frank JA, Zywicke H, Jordan EK, Mitchell J, Lewis BK, Miller B, et al. Magnetic intracellular labeling of mammalian cells by combining (FDA-approved) superparamagnetic iron oxide MR contrast agents and commonly used transfection agents. *Acad Radiol*. 2002 Aug;9 Suppl 2:S484-7.
45. Walczak P, Kedziorek DA, Gilad AA, Lin S, Bulte JW. Instant MR labeling of stem cells using magnetoelectroporation. *Magnet Reson Med*. 2005 Oct;54(4):769-74.
46. Ananta JS, Godin B, Sethi R, Moriggi L, Liu X, Serda RE, et al. Geometrical confinement of gadolinium-based contrast agents in nanoporous particles enhances T1 contrast. *Nat Nanotechnol*. 2010 Nov;5(11):815-21.
47. Key J, Aryal S, Gentile F, Ananta JS, Zhong M, Landis MD, et al. Engineering discoidal polymeric nanoconstructs with enhanced magneto-optical properties for tumor imaging. *Biomaterials*. 2013 Jul;34(21):5402-10.
48. Lee J, Sayed N, Hunter A, Au KF, Wong WH, Mocarski ES, et al. Activation of innate immunity is required for efficient nuclear reprogramming. *Cell*. 2012 Oct 26;151(3):547-58.
49. Wu JC, Chen IY, Sundaresan G, Min JJ, De A, Qiao JH, et al. Molecular imaging of cardiac cell transplantation in living animals using optical bioluminescence and positron emission tomography. *Circulation*. 2003 Sep 16;108(11):1302-5.